Published in final edited form as:
Angew Chem Int Ed Engl. 2011 April 4; 50(15): 3446–3449. doi:10.1002/anie.201006299.

Transformation of an $[Fe(\eta^2\text{-}N_2H_3)]^{1+}$ Species to π-Delocalized $[Fe_2(\mu\text{-}N_2H_2)]^{2+/1+}$ Complexes

Caroline T. Saouma,
Department of Chemistry and Chemical Engineering, California Institute of Technology, 1200 E. California Blvd, Pasadena, CA 91125 (USA), Fax: (+) jpeters@caltech.edu, Homepage: http://jcpgroup.caltech.edu Former address: Department of Chemistry, Massachusetts Institute of Technology, Cambridge, MA, 02139

R. Adam Kinney,
Department of Chemistry, Northwestern University, 2145 Sheridan Road, Evanston, IL, 60208 (USA), Fax: (+) bmh@northwestern.edu Homepage: http://chemgroups.northwestern.edu/hoffman/index.htm

Brian M. Hoffman[Prof.], and
Department of Chemistry, Northwestern University, 2145 Sheridan Road, Evanston, IL, 60208 (USA), Fax: (+) bmh@northwestern.edu Homepage: http://chemgroups.northwestern.edu/hoffman/index.htm

Jonas C. Peters[Prof.]
Department of Chemistry and Chemical Engineering, California Institute of Technology, 1200 E. California Blvd, Pasadena, CA 91125 (USA), Fax: (+) jpeters@caltech.edu, Homepage: http://jcpgroup.caltech.edu Former address: Department of Chemistry, Massachusetts Institute of Technology, Cambridge, MA, 02139

Abstract

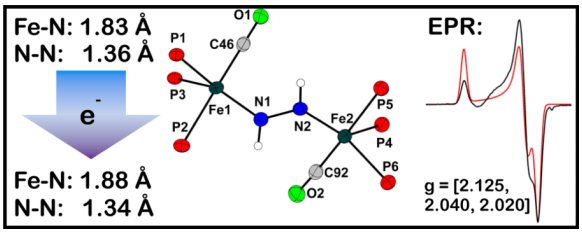

A monomeric iron $Fe(\eta^2\text{-}N_2H_3)$ species has been prepared, and exposure to oxygen yields a diiron complex that features five-coordinate iron centers and an activated bridging diazene ligand (NH=NH). Combined structural, theoretical, and spectroscopic data for the redox pair of complexes $[Fe_2(\mu\text{-}N_2H_2)]^{2+/1+}$ are consistent with 4-center, 4-electron π-delocalized bonding picture across the Fe-NH-NH-Fe core that finds analogy in butadiene and the butadiene anion.

Keywords

Diazene; N_2 fixation; ENDOR; Mixed-valency; Hydrazido

Correspondence to: Brian M. Hoffman; Jonas C. Peters.

Supporting information for this article is available on the WWW under http://www.angewandte.org or from the author. CCDC 795818 – 795821 contain the supplementary crystallographic data for this paper.

Several mechanisms have been proposed to describe the reduction of N_2 to NH_3 at the cofactor of MoFe-nitrogenase.[1] Although experimental evidence is consistent with initial coordination of N_2 through a single metal center of the cofactor,[2] recent DFT studies have pointed to plausible diiron intermediates of the type $Fe_2(N_2H_y)$ (y = 1–4) *en route* to NH_3 formation.[3] In this context, it is noteworthy that diazene[4] and hydrazine[5] are readily reduced to NH_3 by nitrogenase under turnover conditions. Diiron model complexes that feature the $Fe_2(N_2H_y)$ core are therefore of timely interest,[6],[7],[8] especially as a spectral reference point to aid in the interpretation of ENDOR/ESEEM data that is being obtained with the enzymatic system during catalysis.[1d]

Herein we describe the characterization of an $[Fe(\eta^2\text{-}N_2H_3)]^{1+}$ species that gives rise to a binuclear complex with an $[Fe_2(\mu\text{-}N_2H_2)]^{2+}$ core upon exposure to O_2. The latter complex is unique in that combined structural, spectroscopic, and DFT calculations suggest that the bridging 'diazene' is best formulated as $N_2H_2^{2-}$. While this level of diazene activation has been observed in complexes of highly reducing early transition metals[9] it is not well established for the later transition metals, including iron.[7, 10] One-electron reduction of the $[Fe_2(\mu\text{-}N_2H_2)]^{2+}$ complex furnishes the EPR-active mixed-valent $[Fe_2(\mu\text{-}N_2H_2)]^{1+}$ complex, whose electronic structure characterization by combined EPR/ENDOR spectroscopy is described.

Entry to this chemical manifold arises from the addition of N_2H_4 to the iron alkyl precursor $[PhBP_3]FeMe$, **1**, ($[PhBP_3]^- = PhB(CH_2PPH_2)3^-$) in the presence of a suitable trap. We have previously reported that the room temperature reaction between **1** and N_2H_4 quantitatively forms $\{[PhBP_3]Fe\}_2(\mu\text{-}\eta^1\text{:}\eta^1\text{-}N_2H_4)(\mu\text{-}\eta^2\text{:}\eta^2\text{-}N_2H_2)$, with concomitant loss of methane.[7b] A hydrazido complex of the type "$[PhBP_3]Fe(N_2H_3)$" is a plausible thermally unstable intermediate to invoke, and a strong-field trapping ligand was hence pursued. Addition of 1 equiv of N_2H_4 to **1** at −78 °C, followed by addition of 1 equiv of CO, affords orange $[PhBP_3]Fe(\eta^2\text{-}N_2H_3)(CO)$, **2**, in ca. 70 % chemical yield (Scheme 1). Several side reactions compete with formation of **2**, and the crude reaction mixtures invariably contain $\{[PhBP_3]Fe\}_2(\mu\text{-}\eta^1\text{:}\eta^1\text{-}N_2H_4)(\mu\text{-}\eta^2\text{:}\eta^2\text{-}N_2H_2)$,[7b] $[PhBP_3]Fe(CO)_2H$ (see SI), and several other unidentified species. The similar solubilities of $[PhBP_3]Fe(CO)_2H$ and **2** diminish the isolated yield of **2** in analytically pure form.

The solid-state structure of **2** was obtained and indicates that the $N_2H_3^-$ ligand coordinates η_2 to the Fe center (Scheme 1). The Fe-N distances of 1.992(3) and 2.018(3) Å are as expected for coordination of sp^3-hybridized nitrogen to Fe, and are similar to those observed in the related six-coordinate $Fe(\eta^2\text{-}N_2H_4)$ and $Fe(\eta^2\text{-}N_2H_2)$ species.[8] The N1–N2 bond distance of 1.383(3) Å is shorter than that expected for an N-N single bond, but consistent with that of a related $N_2H_3^-$ complex of tungsten.[11]

The ^{15}N NMR spectrum (−75 °C, $[D_8]THF$) of **2** shows a complicated signal centered around 32 ppm, which was fit to obtain chemical shifts and coupling constants (see SI). The NH-*N*H_2 and *N*H-NH_2 chemical shifts are noted at 31.8 ppm and 32.2 ppm, respectively, with $^1J(N,N)$ = 10 Hz. The ^1H NMR spectrum (−75 °C, $[D_8]THF$) of **2** shows three distinct protons for the hydrazido ligand that split into doublets when samples of **2** are prepared with $^{15}N_2H_4$. The N*H*-NH_2 chemical shift is noted at 2.85 ppm ($^1J(N,H)$ = 56 Hz), and the inequivalent NH-N*H*$_2$ protons appear at 6.55 ($^1J(N,H)$ = 86 Hz) and 1.88 ($^1J(N,H)$ = 79 Hz) ppm. The NMR data collectively indicates that the $N_2H_3^-$ ligand is comprised of two sp^3-hybridized nitrogen atoms.

The orange hydrazido(-) complex **2** undergoes decay to the bridged blue diazene complex, $\{[PhBP_3]Fe(CO)\}_2(\mu\text{-}\eta^1\text{:}\eta^1\text{-}N_2H_2)$, **3**, in the presence of 0.5 equiv oxygen (Scheme 1). Other oxidants (e.g., $Pb(OAc)_4$, Cp2Fe$^+$, *p*-quinone), acids (e.g., pyridinium, $FeCl_3$,

$Sm(OTf)_3$), and bases (e.g., N_2H_4, ^{n}BuLi, ^{t}BuN=P(*cyclo*-NC_4H_8)) were canvassed but do not facilitate this transformation. The reaction is solvent dependent and proceeds in benzene but not in THF, perhaps owing to hydrogen bond stabilization of **2** by THF solvent (see SI).

The ^{15}N NMR spectrum of **3** (prepared from ^{15}N- **2**) displays a broad doublet at 292 ppm, indicative of an sp^2-hybridized nitrogen atom. The diazene protons are magnetically inequivalent, and the corresponding $^1H\{^{31}P\}$ NMR spectrum of **3** shows a AA'XX' splitting pattern centered at 9.5 ppm. The chemical shifts of both the H and N atoms of the diazene ligand differ from those observed in the related $\{[PhBP_3]Fe\}_2(\mu\text{-}\eta^1\text{:}\eta^1\text{-}N_2H_2)(\mu\text{-}\eta^2\text{:}\eta^2\text{-}N_2H_2)$ (^{15}N NMR: 407.5, 58.0; ^{1}H NMR: 13.20, 4.16),[7b] and suggest that the extent of diazene activation in the two complexes may be different. Simulation of the $^1H\{^{31}P\}$ spectrum of **3** gives the following coupling constants: $^1J(N,H) = -71.0$ Hz, $^2J(N,H) = -2.1$ Hz, $^3J(H,H) = 14.8$ Hz, and $^1J(N,N) = 9.5$ Hz. The magnitude of the three-bond HH coupling is consistent with a *trans* configuration, and can furthermore be used as a probe for the extent of NN activation.[12] For example, $^3J(H,H) = 28.0$ Hz for $[(CO)_5Cr]_2$(*trans*-μ-N_2H_2),[13] which has an N-N bond distance of 1.25 Å,[14] while $^3J(H,H) = 9.4$ Hz for $[(\eta^5\text{-}C_5Me_4H)_2ZrI]_2$(*trans*-$\mu$-$N_2H_2$), which has an N-N bond distance of 1.414(3) Å.[9b] Hence, the observed $^3J(H,H)$ coupling in **3** is most consistent with a single bond.

The solid-state structure of **3** was obtained and its core atoms are shown in Figure 1 (see SI for complete structure). Both Fe centers have similar metrical parameters, and adopt a distorted trigonal bipyramidal geometry, with the approximate equatorial plane defined by two phosphorous and one nitrogen atom. The two Fe centers are related by a 133° rotation about the Fe-Fe vector. The *trans* protons on the diazene were located in the difference map, and form a planar diazene. However, the Fe-N-N-Fe linkage departs from planarity and features a 20.3° dihedral angle (Figure 1). The average Fe-N bond distance of 1.83 Å in **3** indicates the presence of π-bonding, while the elongated N-N bond distance of 1.362(4) Å establishes a significantly activated diazene unit. This distance is closer to that expected for a $N(sp^2)$-$N(sp^2)$ single bond than that for a double bond (ca. 1.41 Å and 1.24 Å, respectively).[7, 15]

Complex **3** is intensely colored and displays a transition at 716 nm ($\varepsilon = 8500\ M^{-1}\ cm^{-1}$) that is presumably charge transfer in nature by analogy to assignments made for similar bands observed for related dinuclear $M(\eta^1\text{:}\eta^1\text{-}N_2H_2)M$ complexes.[10, 16] The rRaman spectrum of **3** (633 nm excitation) contains an NN vibration at 1060 cm^{-1}, which shifts to 1032 cm^{-1} in samples of ^{15}N-enriched **3** (calculated shift for a diatomic harmonic oscillator: 1023 cm^{-1}). In addition, a second vibration is observed at 665 cm^{-1} (^{15}N: 651 cm^{-1}), which is tentatively assigned as the ν_s(FeN) vibration that couples with the NN vibration. Both of these vibrations are distinct from those measured by Lehnert et al. in an octahedral $Fe_2(\mu\text{-}\eta^1\text{:}\eta^1\text{-}N_2H_2)$ complex (ν(NN) = 1365 cm^{-1}; ν_{as}(FeN) = 496 cm^{-1}),[17] and consistent with appreciably stronger Fe-N and weaker N-N bonds in **3**. The combined structural, NMR, and vibrational data suggest that the diazene bridge in **3** might better be regarded as a dianionic hydrazido, $N_2H_2^{2-}$, as in the lower left resonance form shown in Figure 2B.

Cyclic voltammetry of **3** shows a reversible one-electron reduction to **4** at −1.54 V (vs. Fc/Fc^+), and chemical treatment of **3** with one equiv of Na/Hg in THF cleanly generates the purple mixed-valence $[Fe_2(\mu\text{-}N_2H_2)]^{1+}$ complex, $[\{[PhBP_3]Fe\}_2(\mu\text{-}\eta^1\text{:}\eta^1\text{-}N_2H_2)][Na(THF)_6]$, **4**. Crystals of **4** suitable for XRD were grown by vapor diffusion of cyclopentane into a saturated THF solution of **4**.

The geometry of the $[Fe_2(\mu\text{-}N_2H_2)]^{1+}$ core of **4** is very similar to that of the $[Fe_2(\mu\text{-}N_2H_2)]^{2+}$ core of **3**, as shown by an overlay of their core atoms (Figure 1). Upon reduction the average Fe-N distance *increases* by *ca*. 0.03 Å to 1.88 Å. Consistent with this, the ν_s(FeN) stretch

decreases from 665 cm^{-1} to 643 cm^{-1} (^{15}N: 624 cm^{-1}) upon reduction.[18] The N-N bond distance in **4** is found to exhibit a marginal decrease to 1.342(3) Å upon reduction. These observations are collectively consistent with π-delocalization within the Fe-N-N-Fe core, with the unpaired electron populating an orbital that is predominantly Fe-N antibonding in character.

DFT calculations (see SI) were performed to further probe the electronic structures of both **3** and **4**. The frontier orbitals of **3** are isolobal to those of butadiene, and both the HOMO and LUMO are primarily composed of the Fe-N-N-Fe π-system. The HOMO displays Fe-N π-bonding and N-N π*-bonding character (Figure 2A). The LUMO features N-N π-bonding, and Fe-N π*-bonding character. Population of the LUMO should therefore result in a decrease in the N-N bond distance and an increase in the Fe-N bond distance. However, the SOMO of **4** has only minimal density on the N-N bridge, and so the actual change should be small, as observed. The observation that the reduction of **3** to **4** yields a shortened N-N distance in the N_2H_2 ligand in the present case is consistent with the DFT calculations. A similar result has been provided for a series of $[Mo_2(\mu\text{-}N_2)]^{6+/7+/8+}$ species where formal overall oxidation of the complex leads to a more 'activated' bridging N_2 ligand.[19]

To further probe the electronic structure of the $[Fe_2(\mu\text{-}N_2H_2)]^{1+}$ core of **4**, we turned to EPR/ENDOR spectroscopy. Complex **4** is paramagnetic, with a rhombic $S = ½$ EPR signal (9:1 THF:Me-THF; g = [2.125, 2.040, 2.020]) that remains essentially invariant from 77 K to 2 K. To test the model of a symmetrical, π-delocalized Fe-N-N-Fe core, 35 GHz ^{15}N electron-nuclear double resonance (ENDOR) measurements were performed at 2 K on ^{15}N-**4**.[20] Figure 2C displays ^{15}N ENDOR spectra selected from a 2D field-frequency pattern of ENDOR spectra (ν+ manifold) collected across the EPR envelope of ^{15}N-**4** (see SI). The 2D pattern can be simulated with a single *type* of ^{15}N , having a nearly axial hyperfine coupling tensor, principal values, $A(^{15}N) = +$ [6.7, 5.6, 17.8] MHz, isotropic coupling, $a_{iso}(^{15}N) = +10$ MHz, and anisotropic coupling, $\mathbf{T}(^{15}N) = +$ [−3.3, −4.5, 7.8] MHz (signs have been determined by pulsed ENDOR protocols; see SI).[21] The absence of a Mims ENDOR response associated with a second, more weakly coupled ^{15}N nucleus (not shown),[22] indicates that the two ^{15}N atoms from the bridge are magnetically equivalent and contribute equally to the ENDOR response depicted in Figure 2C, as expected for a delocalized $[Fe_2(\mu\text{-}N_2H_2)]^{1+}$ ground state.

The strong anisotropy of **A** requires that the spin density on the two N atoms is of π character (A_3 parallel to the π-orbital for each N).[23] The positive sign of **A** for ^{15}N indicates that the π spin density on the N-N bridge, $\rho^{\pi}(N)$, is *negative* (see SI), with the anisotropic coupling corresponding to $\rho^{\pi}(N) \sim -0.05$ spins/nitrogen. This small negative spin density on N arises from polarization of doubly-occupied bonding core π orbitals by the large spin density on Fe. The DFT computations on **4** give $\rho^{\pi}(N) \sim -0.36$ spins/nitrogen, which is in satisfactory agreement with experiment given that DFT is well known to overestimate the effects of spin polarization.[24] This finding of rather low spin delocalization onto the bridging nitrogens of **4** illustrates why it is instructive to consider **3** in terms of the butadiene-like resonance structure shown in Figure 2B. The butadiene anion is the corresponding analogue to **4**, and its SOMO is minimally delocalized onto the central atoms. In **4**, delocalization would be decreased further due to the greater electronegativity of N compared to that of Fe.

The orientations of the ^{15}N hyperfine tensors also are informative. The observation of a single, very sharp ^{15}N ENDOR feature at g_1 indicates the g_1 axis is coincident with the N-N vector and normal to the spin-bearing π orbitals on $^{15}N_i$(i = 1, 2). These are expected to be primarily defined by the Fe_i-H_i-N_j (j = 2, 1) planes (Figure 1, bottom right), and thus lie essentially normal to the g_1 axis. Indeed, the 2D ENDOR pattern is satisfactorily simulated

by taking the g_3 axis to bisect the angle between the two Fe_i-H_i-N_j planes, $2\alpha \sim 14°$, and then orienting each $15N_i$ hyperfine tensor along the normal to its plane, which corresponds closely to simply rotating the hyperfine tensors of N1 and N2 around g_1 by equal and opposite angles, $\alpha \sim 7°$ (see Figure 2C, red trace). The data does not define these rotations with precision; not only is agreement with experiment at g_2 improved with $\alpha = 15°$ (see SI), but also the observation of broad features in the ENDOR spectrum at g_3, in contrast to the narrow peak at g_1, suggests that there is a distribution of angles in the frozen solution, likely associated with torsions about the N-N 'single' bond of as little as a few degrees. Overall, the ^{15}N ENDOR results support that **4**, *at 2 K*, contains a π-delocalized Fe-N-N-Fe core, as predicted by DFT computations, with the π-orbital 'twist' indicated by the X-ray structure.

In summary, we have prepared an Fe(η^2-N_2H_3) species, and have shown that the coordinated hydrazido ligand is converted to diazene in the presence of oxygen. The end-on diazene ligands in the $[Fe_2(\mu\text{-}N_2H_2)]^{2+/1+}$ cores of **3** and **4**, are best regarded as '$N_2H_2^{2-}$,' a bonding formulation previously observed for diazene complexes of highly reducing early-transition metals. Combined structural, theoretical, and spectroscopic data for the dinuclear complex **3** indicate the presence of 4-center, 4-electron π-delocalized bonding across the Fe-N-N-Fe diiron μ-diazene core. This picture is consistent with DFT studies, as well as a combined EPR/ENDOR study of its 1-electron reduced congener **4**. This electronic structure, in which the HOMO is N-N π-bonding, provides access to stable diazene complexes in both the $[Fe_2(\mu\text{-}N_2H_2)]^{2+/1+}$ oxidation states. Whether such a fragment arises in the reaction pathway by which nitrogenase reduces N_2 to 2 NH_3 is being explored by detailed comparisons of the results presented here with ENDOR results for nitrogenase intermediates.[25]

Supplementary Material

Refer to Web version on PubMed Central for supplementary material.

Acknowledgments

We acknowledge the NIH (GM-070757, JCP; HL 13531, BMH) and the NSF (MCB0723330, BMH). Funding for the Caltech NMR facility has been provided in part by the NIH (RR 027690) and funding for the MIT Department of Chemistry Instrumentation Facility has been provided in part by the NSF (CHE-0234877). The Betty and Gordon Moore Foundation supports the Molecular Observatory at Caltech. C.T.S. is grateful for an NSF graduate fellowship. Alec Durrell and Jens Kaiser provided guidance for rRaman and XRD experiments, respectively.

References

1. (a) Howard JB, Rees DC. Proc. Natl. Acad. Sci. U.S.A. 2006; 103:17088–17093. [PubMed: 17088547] (b) Peters, JC.; Mehn, MP. Activation of Small Molecules. Tolman, WB., editor. Wiley-VCH; 2006. p. 81-119.(c) Schrock RR. Angew. Chem. Int. Ed. 2008; 47:5512–5522.(d) Hoffman BM, Dean DR, Seefeldt LC. Acc. Chem. Res. 2009; 42:609–619. [PubMed: 19267458]
2. Barney BM, Lukoyanov D, Igarashi RY, Laryukhin M, Yang TC, Dean DR, Hoffman BM, Seefeldt LC. Biochemistry. 2009; 48:9094–9102. [PubMed: 19663502]
3. (a) Hinnemann B, Nørskov JK. J. Am. Chem. Soc. 2004; 126:3920–3927. [PubMed: 15038746] (b) Kästner J, Blöchl PE. J. Am. Chem. Soc. 2007; 129:2998–3006. [PubMed: 17309262] (c) Dance I. Dalton Trans. 2010; 39:2972–2983. [PubMed: 20221528]
4. Barney BM, McClead J, Lukoyanov D, Laryukhin M, Yang TC, Dean DR, Hoffman BM, Seefeldt LC. Biochemistry. 2007; 46:6784–6794. [PubMed: 17508723]
5. Barney BM, Yang T-C, Igarashi RY, Dos Santos PC, Laryukhin M, Lee H-I, Hoffman BM, Dean DR, Seefeldt LC. J. Am. Chem. Soc. 2005; 127:14960–14961. [PubMed: 16248599]
6. For Fe(N_2H_3) complexes see: (a) Crossland JL, Balesdent CG, Tyler DR. Dalton Trans. 2009:4420–4422. [PubMed: 19488434] (b) Lee YH, Mankad NP, Peters JC. Nature Chemistry. 2010; 2:558–565.

7. For end-on diazene coordination see: (a) Sellmann D, Sutter J. Acc. Chem. Res. 1997; 30:460–469. (b) Saouma CT, Müller P, Peters JC. J. Am. Chem. Soc. 2009; 131:10358–10359. [PubMed: 19722612]
8. For side-on diazene coordination see: Field LD, Li HL, Dalgarno SJ, Turner P. Chem. Commun. 2008:1680–1682. (b) ref. 7b
9. (a) Churchill MR, Li YJ, Blum L, Schrock RR. Organometallics. 1984; 3:109–113.(b) Bernskoetter WH, Pool JA, Lobkovsky E, Chirik PJ. J. Am. Chem. Soc. 2005; 127:7901–7911. [PubMed: 15913380]
10. Fujisawa K, Lehnert N, Ishikawa Y, Okamoto K-i. Angew. Chem. Int. Ed. 2004; 43:4944–4947.
11. Schrock RR, Liu AH, O'Regan MB, Finch WC, Payack JF. Inorg. Chem. 1988; 27:3574–3583.
12. Cooper MA, Manatt SL. J. Am. Chem. Soc. 1969; 91:6325–6333.
13. Smith MR, Cheng TY, Hillhouse GL. J. Am. Chem. Soc. 1993; 115:8638–8642.
14. Huttner G, Gartzke W, Allinger K. Angew. Chem., Int. Ed. Engl. 1974; 13:822–823.
15. Allman, R. The Chemistry of the Hydrazo, Azo, and Azoxy Groups. Patai, S., editor. New York: Wiley; 1975. p. 28
16. Lehnert N, Wiesler BE, Tuczek F, Hennige A, Sellmann D. J. Am. Chem. Soc. 1997; 119:8869–8878.
17. Lehnert N, Wiesler BE, Tuczek F, Hennige A, Sellmann D. J. Am. Chem. Soc. 1997; 119:8879–8888.
18. The presence of an additional CT band precluded our ability to obtain strong resonance enhancement, and the NN stretch could hence not be reliably located for **4**
19. Curley JJ, Cook TR, Reece SY, Müller P, Cummins CC. J. Am. Chem. Soc. 2008; 130:9394–9405. [PubMed: 18576632]
20. The ENDOR response for a ^{15}N nucleus (I = 1/2) in which $A > \nu_n$ is given by the equation $\nu = A/2 \pm \nu_n$. Mims and Davies 35 GHz pulsed ENDOR measurements: Schweiger A, Jeschke G. Principles of Pulse Electron Paramagnetic Resonance. 2001Oxford, UKOxford University Press
21. (a) Yang T-C, Hoffman BM. Journal of Magnetic Resonance. 2006; 181:280–286. [PubMed: 16777447] (b) Doan PE. Journal of Magnetic Resonance. 2010
22. Tierney DL, Huang H, Martásek P, Roman LJ, Silverman RB, Hoffman BM. J. Am. Chem. Soc. 2000; 122:7869–7875.
23. Carrington, A.; McLachlan, AD. Introduction to Magnetic Resonance. Ney York: Harper & Row; 1967. p. 94
24. Rado0ń M, Broclawik E, Pierloot K. The Journal of Physical Chemistry B. 2010; 114:1518–1528. [PubMed: 20047294]
25. Such comparisons are not straightforward because the Fe ions of nitrogenase presumed to bind substrate-derived species form part of the spin-coupled catalytic [Fe7Mo] molybdenum-iron cofactor.

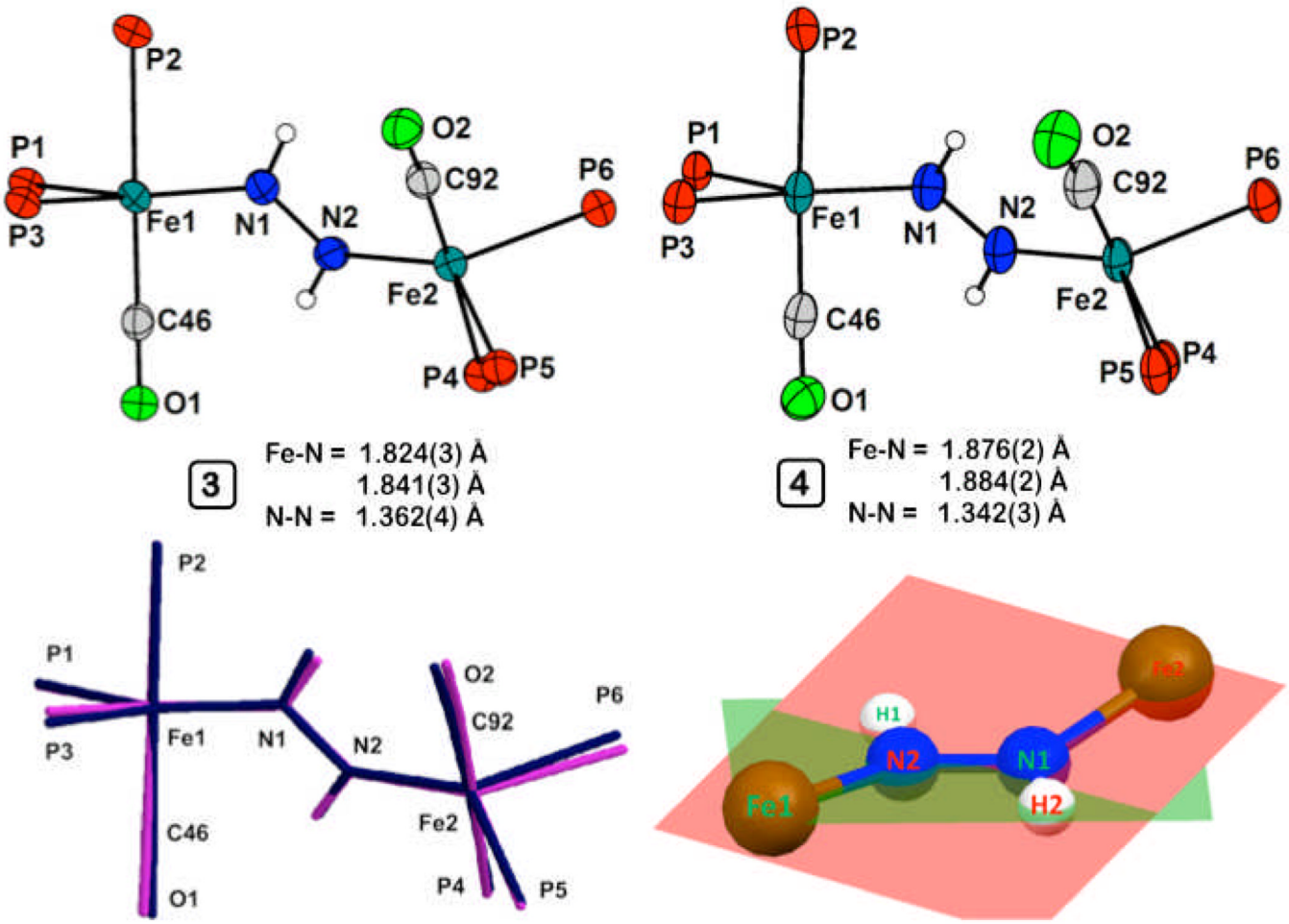

Figure 1.

Displacement ellipsoid (50 %) representations of the core atoms of **3** (left, top) and **4** (right, top), and an overlay of their core atoms (bottom, left; black, **3**; gray, **4**), and a representation showing the twist of the Fe-N-N-Fe linkage of **4** (bottom, right).

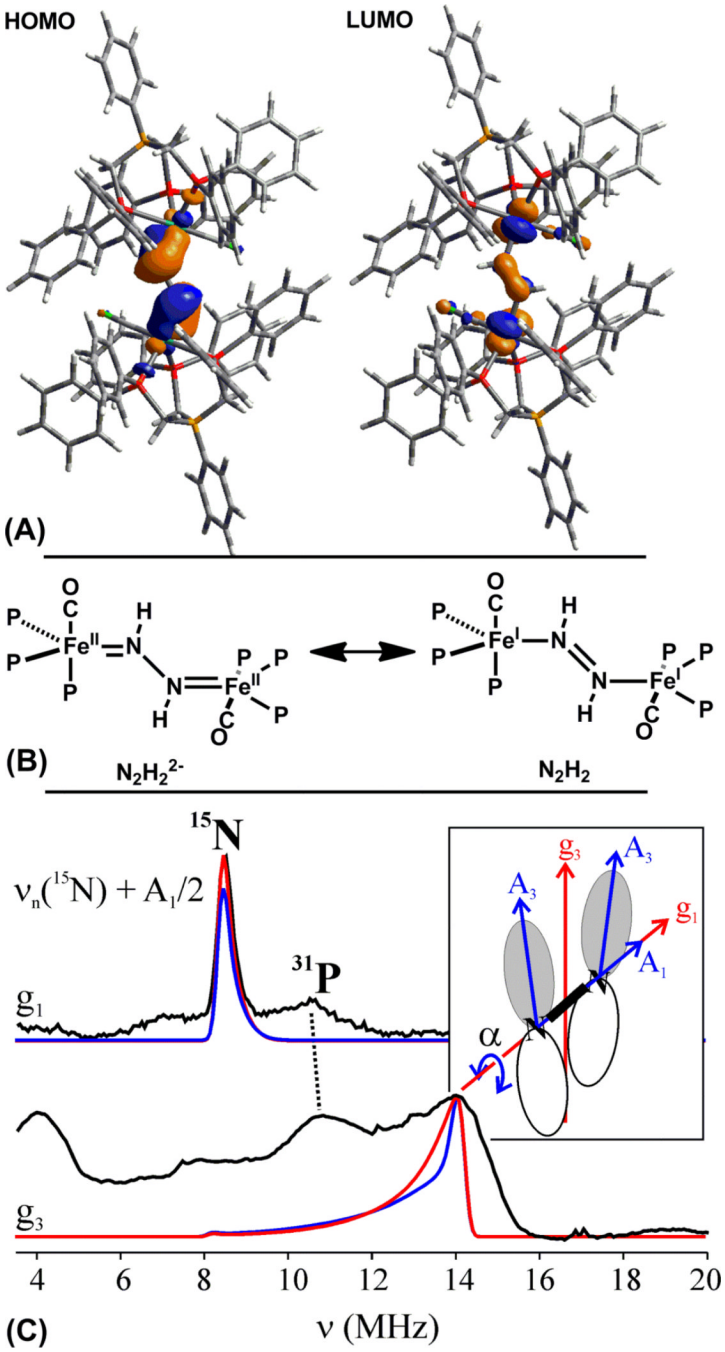

Figure 2.

(A) HOMO and LUMO of **3** (isocontour = 0.04); see SI for computational details. (B) Plausible resonance contributors to the electronic structure of **3**. (C) 35 GHz Davies ^{15}N pulsed ENDOR spectra (black traces; ν+ manifold ($\nu_+ = \nu_n + A/2$)) from ^{15}N-**4** at the indicated g values. Simulations (red, $\alpha = \pm 7°$) use hyperfine and g tensors given in the text (see SI); the ENDOR linewidth in the g_3 simulation is greater than that for g_1, as would be required by a distribution of α, see text.

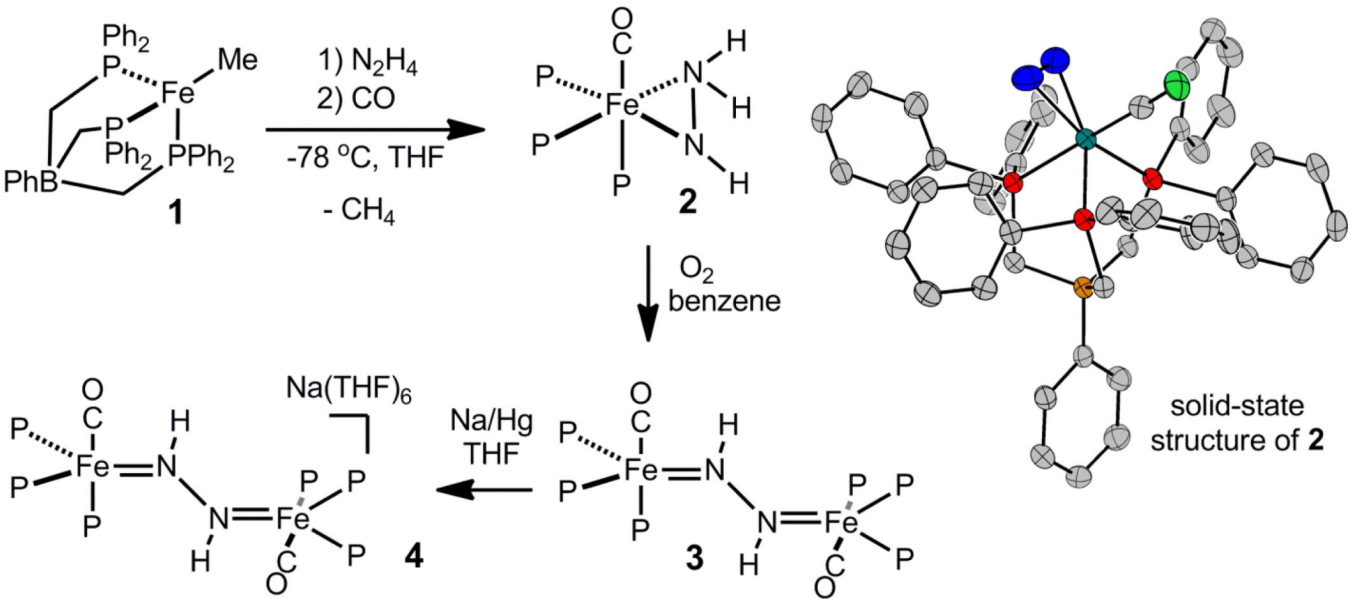

Scheme 1.